DEUTSCHES ELEKTRONEN-SYNCHROTRON DESY

DESY 71/19
April 1971

DESY-Bibliothek
-5. MAI 1971

Preliminary Results on Coincidence Measurements for Electroproduction in the Deep Inelastic Region

by

F. W. Brasse, W. Fehrenbach, W. Flauger, K. H. Frank, J. Gayler
V. Korbel, J. May and P. D. Zimmermann

Deutsches Elektronen-Synchrotron DESY, Hamburg

and

E. Ganßauge

Physikalisches Institut der Universität Marburg

2 HAMBURG 52 · NOTKESTIEG 1

Preliminary Results on Coincidence Measurements for Electroproduction in the Deep Inelastic Region

by

F. W. Brasse, W. Fehrenbach, W. Flauger[+], K. H. Frank, J. Gayler
V. Korbel, J. May and P. D. Zimmerman[++]

Deutsches Elektronen-Synchrotron DESY, Hamburg

and

E. Ganßauge
Physikalisches Institut der Universität Marburg

[+]Present address: CERN, Geneva
[++]Present address: University of Los Angeles, Los Angeles, USA

ABSTRACT

In the deep inelastic region of electroproduction coincidence measurements for the reactions $e + p \rightarrow e + p + M_x$ and $e + p \rightarrow e + \pi^+ + M_y$ have been made. Preliminary results for the production cross sections by virtual photons $d^2\sigma/d\Omega dP_{p,\pi}$ and $d^2\sigma/d\Omega dM_{x,y}$ are given.

Inelastic electron proton scattering has been investigated very extensivly at different laboratories by measuring the total cross section for the absorption of virtual photons on protons as a function of the four momentum transfer q^2 to the final hadronic system and of its mass W. In the deep inelastic region, which is the region of W above the main nucleon resonances (W > 2 GeV) and of q^2 above 1 $(GeV/c)^2$, two main results were found: 1) the cross section is large compared with that for elastic scattering or for the production of the first nucleon resonance, 2) the structure functions W_1 and W_2 depend only on a combination of the two variables q^2 and W and not on both independently. In order to understand these results it is necessary to decompose the total cross section in special reactions.

We have measured the following classes of reactions

$$e + p \rightarrow e + p + \text{anything with missing mass } M_x$$

and

$$e + p \rightarrow e + \pi^+ + \text{anything with missing mass } M_y$$

by detecting electron and proton respectively pion in coincidence. Momenta and angles of the detected particles were measured so that the four momentum vector of the virtual photon and of the undetected system was known.
The hadron was detected in the direction of the virtual photon. The momentum of the proton or of the pion was varied across a large range to vary the missing mass for the rest system. W and q^2 were chosen such that the conditions for deep inelastic region, as indicated by the total cross section, are fullfilled.

The apparatus, which was used for this experiment, is shown in Fig. 1. The external electron beam hits a 9 cm liquid hydrogen target, passes a secondary emission monitor and a beam position monitor and is stopped in a Farady cup. The scattered electrons are measured in a double focussing spectrometer, which was already used in a previous experiment.[1] Electrons are identified by a Cerenkov and a shower counter. The protons and pions are detected in a spectrometer, which consists of three half quardrupoles with the same polarity. The particles are focused in the vertical plane. Two hodoscopes with a space resolution of 3 mm for each, measure the vertical angle and the momentum. The horizontal angle is measured by one of the trigger counters, which devide the small horizontal acceptance into three parts. A gas threshold Cerenkov counter separates pions from heavier particles (mainly protons) for momenta larger than 900 MeV/C.

The shower counter discriminates against positrons and is used for protons with low momentum as a range counter. In both trigger counters and in the Cerenkov counter the time of flight of the hadrons is measured with respect to that of the electron. This information is used to subtract random coincidences between the two arms and to separate pions from protons below 900 MeV/c. The lowest proton momentum, which can be detected, is approximately 400 MeV/c. At the entrance of the first quadrupole of the hadron spectrometer 60 cm of lead are put in the horizontal plane to prevent direct sight between the hodoscopes and the target. Since we did not want to exclude the very forward direction with respect to the virtual photon, the spectrometer is tilted towards the horizontal plane by about 30 mrad.

The acceptance of the electron arm is 0.95 msr and 10 % in momentum. The hadron arm has a very large momentum acceptance. Far outside of the central value however the resolution is no longer sufficient and the solid angle acceptance is small. The range, which was actually used, goes from -34% to +52 %. Here the solid angle varies from 0.4 msr to 1.1 msr at the central momentum and to 0.5 msr at the +52 % limit. The resolution in momentum is approximately 2% FWHM in this range. The angular resolution is about 0.1° FWHM for both directions.

The main kinematical parameters, at which the measurements were made, are listed in Table 1. The values are averaged according to the acceptance of the electron spectrometer.

For the calculation of cross sections of the form $\frac{d^4\sigma}{dE' d\Omega_e dP d\Omega}$

the acceptances $\Delta\Omega \cdot \Delta P$ of the two spectrometers have been determined by Monte Carlo methods. The counting rates have been corrected for random coincidences. The correction goes from zero at the high momenta to at most 50 % at the lowest momenta. Radiative corrections have not been applied so far. We believe however that the distributions will not be changed significantly by the corrections. The elastic radiative tail cannot contribute to the proton spectrum above 400 MeV/c.

In Fig. 2 the cross section for the production of protons with momentum p by virtual photons in the forward direction

$$\frac{d^2\sigma}{d\Omega_p dP_p} = \frac{1}{\Gamma_t} \cdot \frac{d^4\sigma}{dE' d\Omega_e dP_p d\Omega_p}$$

is shown as a function of the laboratory momentum of the proton. Γ_t is defined in the usual way to separate out the electron kinematics.[2] Also shown is the scale of the averaged momentum of the proton in the center of mass system of all outgoing hadrons. The cross section increases with decreasing momentum and shows a broad maximum at a laboratory momentum of about 1.5 GeV/c. Below this range the cross section decreases with decreasing momentum. At the maximum the center of mass momentum is around zero. In principle it is caused by large values of $\Delta\Omega_{CM}/\Delta\Omega$ in this range.

At large momenta the cross section is very small. This is in contradiction to expectations from the fieldtheoretical parton model of Drell, Levy and Yan.[3] In this model spin 1/2 hadrons in the direction of the virtual photon, with a momentum of the order of the three momentum of the virtual photon, which is in our case 4 GeV/c, are expected to contribute to a large extent to the total photoabsorbtion cross section. The measured total spectrum contains approximately 0.1% of the total cross section, which has been measured at the same time with the electron arm alone. In the spirit of Drell et al., we assumed that for 50% of the total cross section a proton is emitted with a longitudinal momentum larger than 2 GeV and a transverse momentum normally distributed around zero with an expectation value $\sqrt{\langle p_\perp^2 \rangle} = 0.35$ GeV. In this case the proton spectrum above 2 GeV should contain more than 0.4% of the total cross section. This should be compared with about 0.04%, which is the measured part of the total cross section with momenta above 2 GeV.

Comparison with the corresponding, but preliminary spectrum from photoproduction[4] for an energy $E_\gamma = 2.8$ GeV shows however, that in the electroproduction case with $q^2 = 1.15$ GeV^2 one has in relation to the total cross sections about two times more protons in the forward direction than in photoproduction.

The corresponding missing mass spectrum for the detected protons is shown in Fig.3. Here only the protons, which are in the forward direction in the CM-system, are used. The steep increase at the very high missing mass values is due to the increase of dP/dM_x. The cross section in the region of backward produced single π^0, η and ρ, not shown in Fig.3, is very small (the spectrum was measured to highest possible momentum of 4.3 GeV, corresponding to $M_x = m_\pi$). Between $M_x = 1.0$ and 1.1 GeV we see an excess of the cross section. Since we have not separated K-mesons from protons, it is possible that we see here electroproduction of Λ or Σ. The missing mass calculated for having detected K-mesons instead of protons is in agreement with both reactions.

The results for the pions are shown in Figs.4 and 5, where $d^2\sigma/d\Omega dP_\pi$ and $d^2\sigma/d\Omega dM_y$ are plotted against momentum and missing mass. The momentum spectrum is rather flat. Here the amount of pions which are produced in the forward direction is at $q^2 = 1.15\ (\mathrm{GeV}/c)^2$ about the same as at $q^2 = 0$, again taking into account the different total cross sections.[4] The missing mass spectrum shows the single pion production in forward direction and perhaps also Δ^0-production. The cross section is slowly increasing across the range of the higher resonances and reaches quite high values at the end of the possible missing mass range, where the detected pions are almost at rest in the CM-system.

We want to emphasize that all data are preliminary, since radiative corrections are not yet applied.

Acknowledgement:

We thank Dr. H. Dorner for his help during the early stage of the experiment in preparing the PDP-programs.

References

1) W. Albrecht et al.: Nuclear Phys. B 25 (1970), 1

2) For definition of Γ_t see for example: F.W. Brasse et al., Nuovo Cim. 55 A (1968), 679

3) S.D. Drell, D.J. Levy and Tung-Mow Yan: Phys Rev. Lett. 22,744 (1969) and SLAC PUB 645 (1969)

4) Private communication by G. Wolf. The data are from a hydrogen bubble chamber experiment of the SLAC-Berkely-Tufts Collaboration using a Compton backscattered monochromatic γ-beam.

Figure Captions:

Fig.1: The experimental apparatus

Fig.2: The photoproduction cross section $\frac{d^2\sigma}{d\Omega dP}$ for protons in the direction of the virtual and real photon as a function of the momentum of the proton.

Fig.3: The cross section $\frac{d^2\sigma}{d\Omega dM_x}$ for the proton spectrum of Fig.2 produced by virtual photons with $P_p^{CM} > 0$ only.

Fig.4: The photoproduction cross section $\frac{d^2\sigma}{d\Omega dP}$ for positive pions in the direction of the virtual and real photon as a function of the momentum of the pion.

Fig.5: The cross section $\frac{d^2\sigma}{d\Omega dM_y}$ for the pion spectrum of Fig. 4 produced by virtual photons.

Table I: Kinematical values of measurement

Energy of primary electron		$E = 6.5$ GeV
Energy of secondary electron		$E' = 2.64$ GeV $\pm$ 5 %
Scattering angle of electron		$\theta = 15.0^{o}$
Angle of virtual photon		$\psi = 10^{o}$
Momentum transfer to hadronic system		$q^2 = 1.15\ (\mathrm{GeV})^2$
Mass of the hadronic system		$W = 2.63$ GeV
Three momentum of the virtual photon		$\lvert\vec{q}\rvert = 4.0$ GeV
Equivalent photonenergy		$K = 3.2$ GeV
Scaling variable	$2M(E-E')/q^2 =$	$\omega = 6$
Polarization of virtual photon		$\varepsilon = 0.7$

Fig. 1

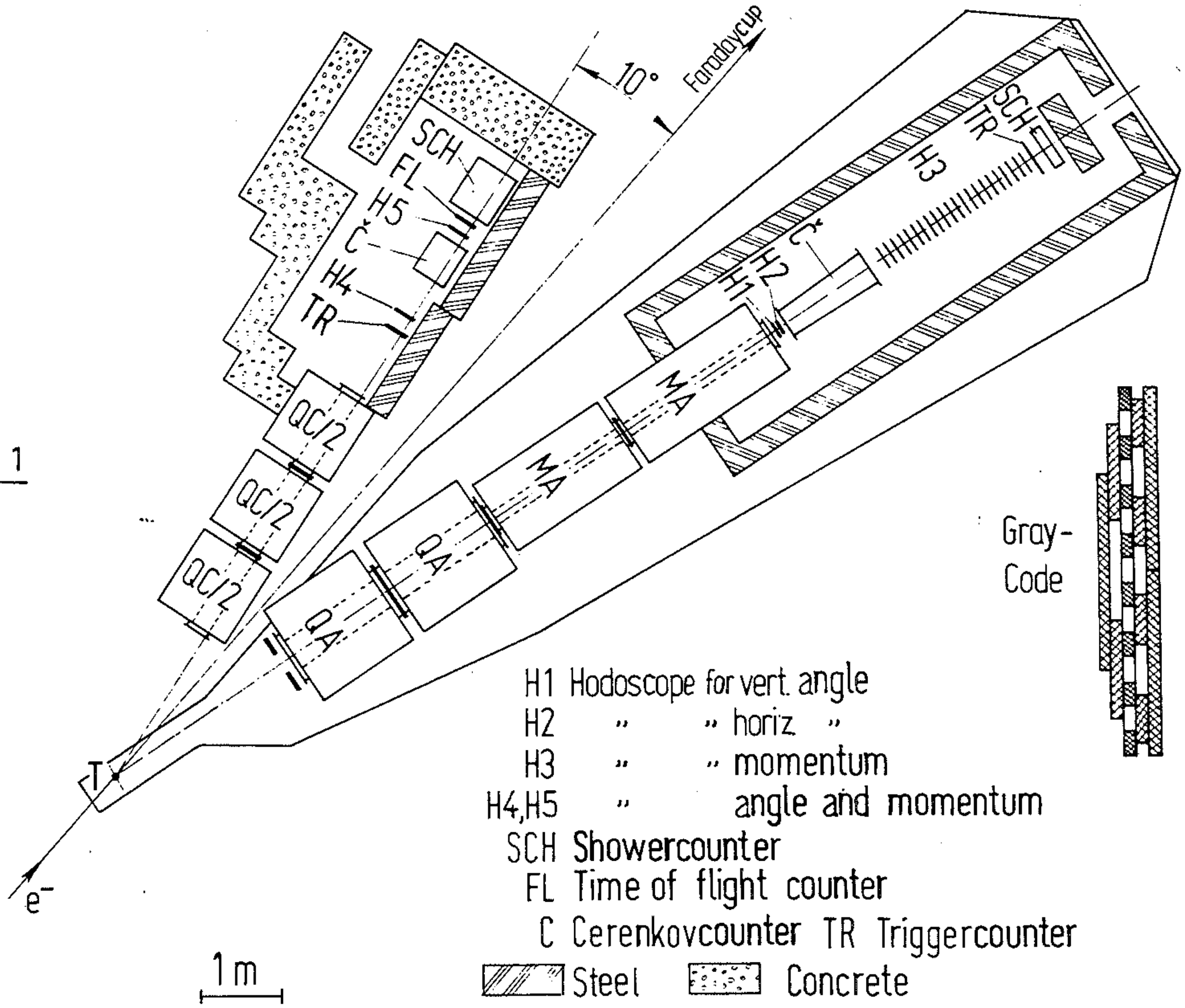

10°
Faradaycup
SCH
FL
H5
Č
H4
TR
QC/2
QC/2
QC/2
QA
QA
QA
MA
MA
MA
SCH
TR
H3
Č
H2
H1
T
e⁻
Gray-
Code
H1 Hodoscope for vert. angle
H2 " " horiz. "
H3 " " momentum
H4,H5 " angle and momentum
SCH Showercounter
FL Time of flight counter
C Cerenkovcounter TR Triggercounter
Steel
Concrete
1 m

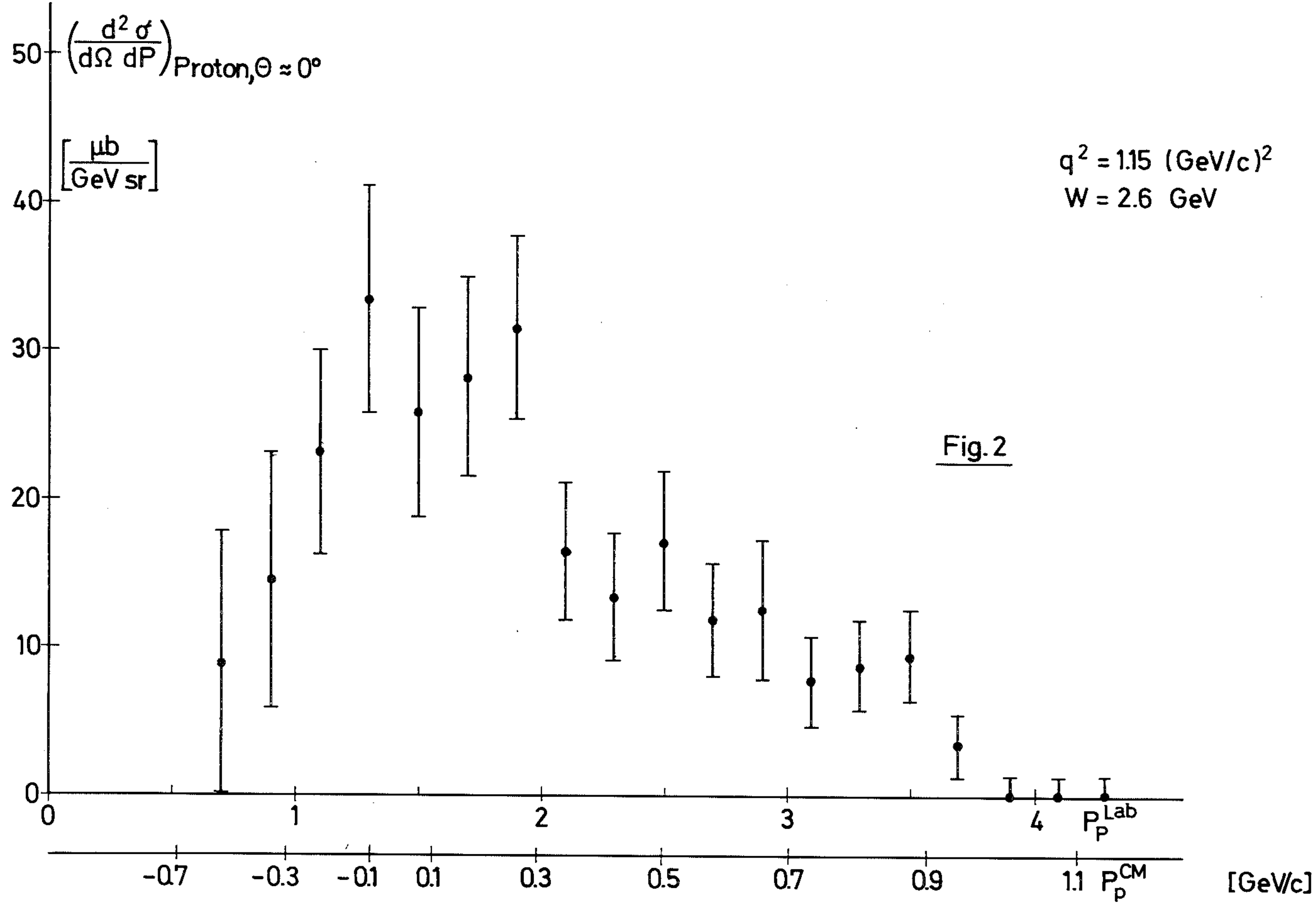

$\left(\frac{d^2\sigma}{d\Omega\, dP}\right)_{Proton, \Theta \approx 0°}$
$\left[\frac{\mu b}{GeV\, sr}\right]$
50
40
30
20
10
0
0
1
2
3
4
P_P^{Lab}
-0.7
-0.3
-0.1
0.1
0.3
0.5
0.7
0.9
1.1
P_p^{CM}
[GeV/c]
$q^2 = 1.15\ (GeV/c)^2$
W = 2.6 GeV

Fig. 2

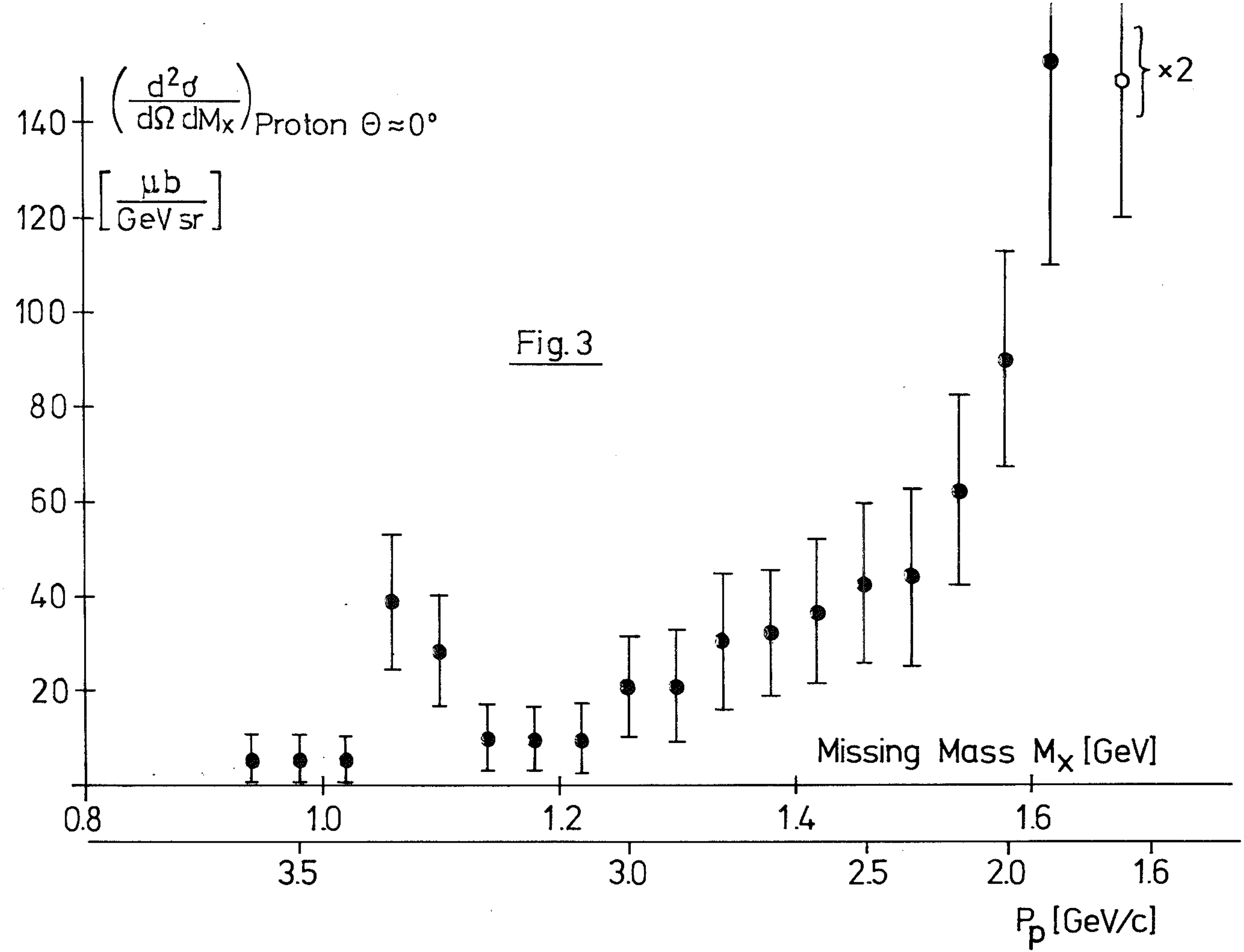

$\left(\frac{d^2\sigma}{d\Omega\, dM_x}\right)$ Proton $\Theta \approx 0°$
$\left[\frac{\mu b}{GeV\ sr}\right]$
140
120
100
80
60
40
20
× 2
Missing Mass M_X [GeV]
0.8
1.0
1.2
1.4
1.6
3.5
3.0
2.5
2.0
1.6
P_p [GeV/c]

Fig. 3

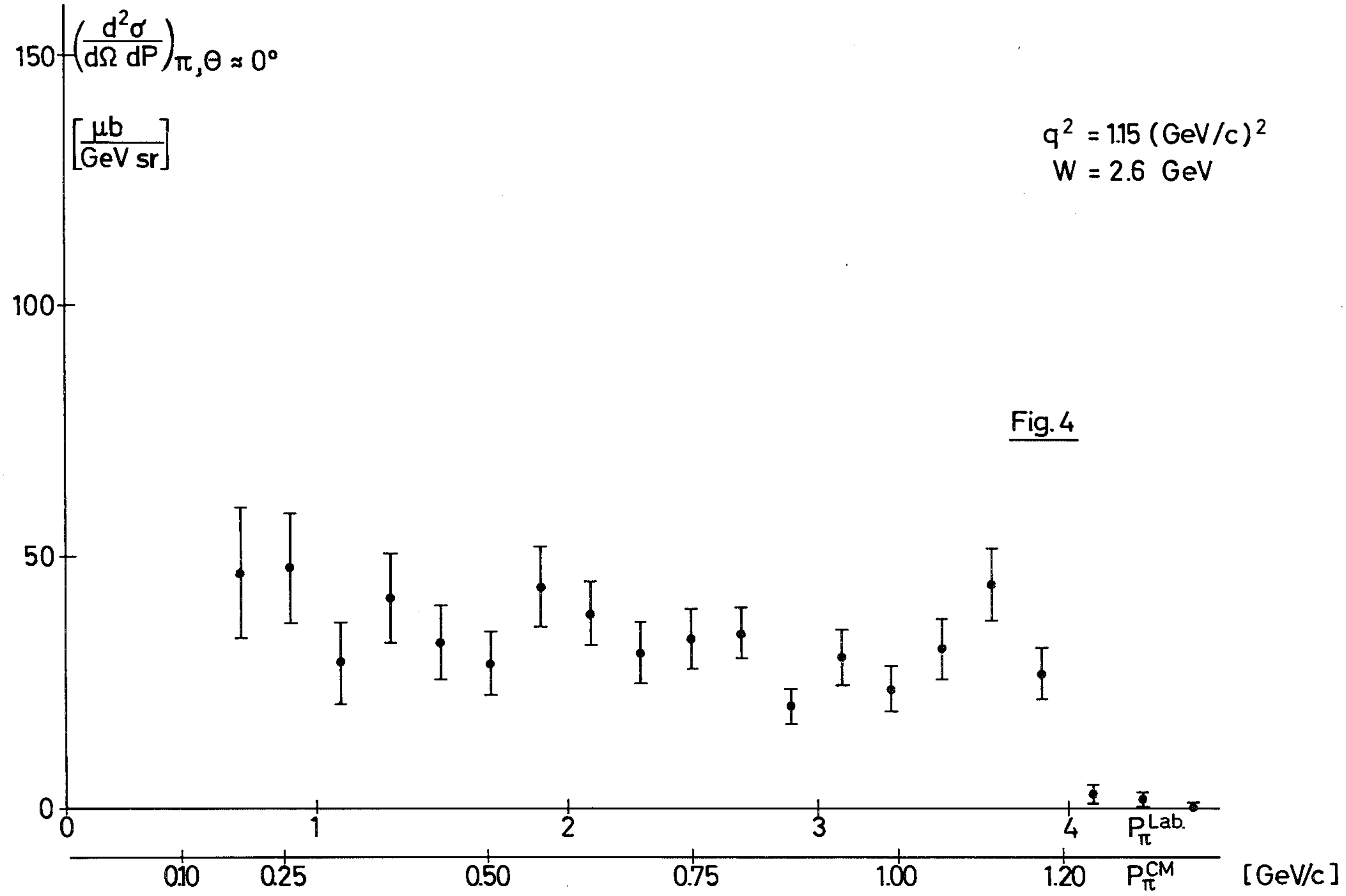

150
100
50
0
$\left(\frac{d^2\sigma}{d\Omega\, dP}\right)_{\pi,\Theta \approx 0°}$
$\left[\frac{\mu b}{GeV\ sr}\right]$
$q^2 = 1.15\ (GeV/c)^2$
W = 2.6 GeV
0
1
2
3
4
$P_\pi^{Lab.}$
0.10
0.25
0.50
0.75
1.00
1.20
P_π^{CM}
[GeV/c]

Fig. 4

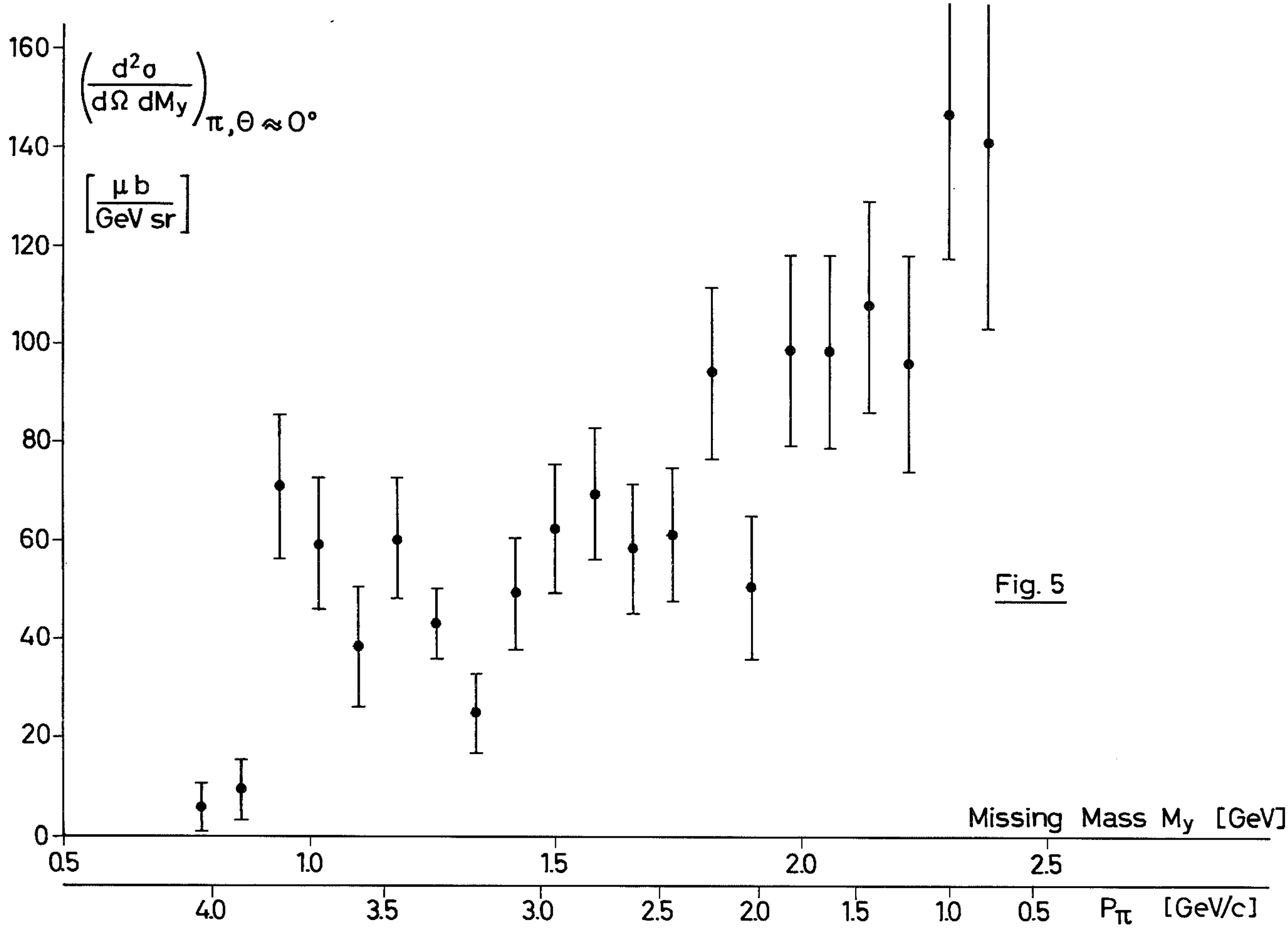

$\left(\frac{d^2\sigma}{d\Omega\, dM_y}\right)_{\pi,\Theta\approx0°}$
$\left[\frac{\mu b}{GeV\ sr}\right]$
160
140
120
100
80
60
40
20
0
Missing Mass M_y [GeV]
0.5
1.0
1.5
2.0
2.5
4.0
3.5
3.0
2.5
2.0
1.5
1.0
0.5
P_π [GeV/c]

Fig. 5